arXiv:cond-mat/0209061v2 [cond-mat.supr-con] 6 Dec 2002

Checkerboard local density of states in striped domains pinned by vortices

Brian Møller Andersen, Per Hedegård and Henrik Bruus*
Ørsted Laboratory, Niels Bohr Institute for APG, Universitetsparken 5, DK-2100 Copenhagen Ø Denmark
**Mikroelektronik Centret, Technical University of Denmark, DK-2800 Lyngby*
(December 2002)

We discuss recent elastic neutron scattering and scanning tunneling experiments on High-T_c cuprates exposed to an applied magnetic field. Antiferromagnetic vortex cores operating as pinning centers for surrounding stripes is qualitatively consistent with the neutron data provided the stripes have the antiphase modulation. Within a Green's function formalism we study the low energy electronic structure around the vortices and find that besides the dispersive quantum interference there exists a non-dispersive checkerboard interference pattern consistent with recent scanning tunneling measurements. Thus both experiments can be explained from the physics of a single CuO_2 plane.

PACS numbers: 74.72.-h, 74.25.Ha, 74.25.Jb

The competing orders in the High-T_c cuprates remain a strong candidate for explaining some of the unusual features of these doped Mott insulators[1–5]. The competition between superconducting order and antiferromagnetic order has recently attracted a large amount of both experimental and theoretical attention. In particular, experiments in the mixed state have revealed an interesting coexistence of these order parameters.

Elastic neutron scattering results on $La_{2-x}Sr_xCuO_2$ (x=0.10) have shown that the intensity of the incommensurate peaks in the superconducting phase is considerably increased when a large magnetic field is applied perpendicular to the CuO_2 planes[6]. This enhanced intensity corresponds to a spin density periodicity of eight lattice constants $8a_0$ extending far outside the vortex cores. Similar results have been obtained for the related material La_2CuO_{4+y}[7]. Nuclear magnetic resonance (NMR) experiments have shown evidence for antiferromagnetism in and around the vortex cores of near-optimally doped $Tl_2Ba_2CuO_{6+\delta}$[8]. Furthermore, muon spin rotation measurements from the mixed state of $YBa_2Cu_3O_{6.50}$ find static antiferromagnetism in the cores[9]. Consistent with these findings scanning tunneling microscopy (STM) measurements performed on the surface of $YBa_2Cu_3O_{7-\delta}$ and $Bi_2Sr_2CaCu_2O_{8+x}$[10,11]have revealed very low DOS inside the vortex cores[12–14]. Thus, there is increasing evidence for antiferromagnetic correlations in the vortex cores of the under- and optimally-doped regime of the hole doped cuprates. More recent STM measurements of slightly overdoped $Bi_2Sr_2CaCu_2O_{8+x}$ have shown a checkerboard halo of the local density of states (LDOS) around the vortex cores[15]. This LDOS modulation observed at low energy $|\omega| < 12$ meV was found to have half the period of the spin density wave (SDW) observed by neutron scattering (i.e. four lattice constants $4a_0$), and to be oriented along the crystal axes of the Cu-O plane. The neutron experiments have been analysed within phenomenological models that assume close proximity to a quantum phase transition between ordinary superconductivity and a phase with antiferromagnetism or a phase where superconductivity coexists with SDW and charge density wave (CDW) order[5,16–18]. In these models the suppression of the superconducting order inside the vortex cores allows the competing magnetic order to arise. Demler *et al.*[17] found that around the vortices the circulating supercurrents can similarly weaken the superconductivity and induce a SDW.

The field-induced checkerboard LDOS pattern in the mixed state has been recently considered within the framework of several models[18–23]. In this paper we add to the discussion by calculating the LDOS in regions where a d-wave superconductor has been perturbed by induced magnetism. First, however, we note that a checkerboard *spin* modulation is inconsistent with the elastic neutron scattering experiments by Lake *et al.*[6] on $La_{2-x}Sr_xCuO_2$ (x=0.10). For example, assuming that the checkerboard CDW is intrinsic to the Cu-O planes where it gives rise to a static SDW checkerboard pattern (Fig. 1a), the expected neutron diffraction pattern is shown in Fig. 1b.

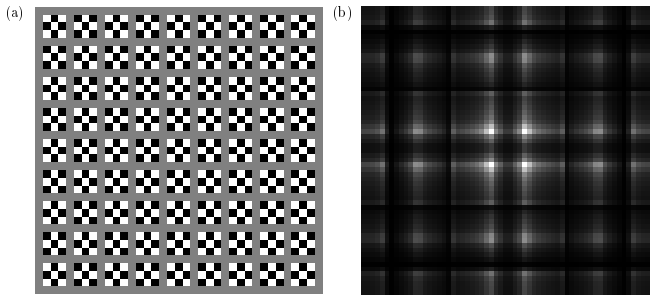


FIG. 1. a) Real space picture of the spin structure in a checkerboard spin geometry. Black (white) represent spin up (down) while gray reveals the superconducting background. In order to simulate the induced incommensurability each island of antiferromagnetic spins is out of phase with its nearest neighbor. b) Fourier spectrum of the spin checkerboard structure shown in a).

As is evident there is a 45 degree rotation of the four main incommensurate peaks and a plaid pattern of the higher harmonics. The rotated incommensurability (with

the correct absence of an increased signal at (π, π)) shows that this spin structure does not apply to LSCO for doping levels close to $x = 0.10$. It is interesting to note that a rotation of the incommensurable peaks at low dopings ($x < 0.055$, close the insulator-superconductor phase transition) has been observed in LSCO[25]. However, there is no simple way to create an antiphase spin geometry without frustrating the spins at low dopings where droplets of charge in an antiferromagnetic background is the expected situation[26]. However, this might be possible in the highly overdoped regime where the droplets have been inverted to separate magnetic islands. In that case a 45 degree rotation of the incommensurable peaks would be consistent with a checkerboard spin pattern. In this light it would be very interesting to perform an experiment similar to Lake *et al.*[6] on highly overdoped LSCO. In the case of a connected antiferromagnetic background one would also expect a large weight at (π, π).
The physical picture we have in mind is presented in figure 2a. In this real space picture an antiferromagnetic core (center) has pinned a number of surrounding stripes.

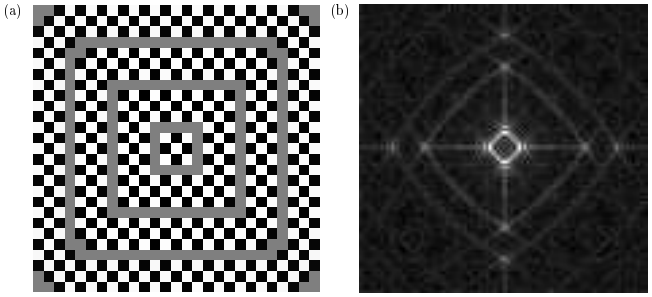


FIG. 2. a) The idealized version of a real space spin configuration consistent with our physical picture. b) Fourier spectrum of the spin density order from a). Almost all the induced weight is located in the four incommensurable peaks.

This pinning effect of SDW by magnetic vortex cores is a well-known effect from numerical studies[21].
Both experimentally[28] and theoretically[1,3,5,29] we expect an antiphase modulation of the induced antiferromagnetic ring domains. Indeed as seen in Figure 2b the related diffraction pattern is qualitatively consistent with measurements by Lake *et al.*[6] of enhanced intensity at the incommensurate points.
Without an applied magnetic field, only disorder can produce a similar pinning effect of the fluctuating stripes[27]. In addition to the creation of more pinning centers when applying a magnetic field, the single site impurities are expected to pin much weaker than the large "impurities" created by the flux lines. This is qualitatively consistent with the measurements by Lake *et al.*[6] of the temperature dependence of the increased magnetic signal for different magnetic field strengths.
This leads to the question of the electronic structure around extended magnetic perturbations in d-wave superconductors. The many experiments indicating coexistence of d-wave superconductivity and antiferromagnetism mentioned above motivate studies of simple models that enable one to calculate the LDOS in such regions. The model Hamiltonian defined on a 2D lattice is given by

$$\hat{H}^0 = -\sum_{\langle n,m\rangle\sigma} t_{nm}\hat{c}^\dagger_{n\sigma}\hat{c}_{m\sigma} - \mu\sum_{n\sigma}\hat{c}^\dagger_{n\sigma}\hat{c}_{n\sigma} + \sum_{\langle n,m\rangle}\left(\Delta_{n,m}\hat{c}^\dagger_{n\uparrow}\hat{c}^\dagger_{m\downarrow} + H.c.\right) \quad (1)$$

$$\hat{H}^{int} = \sum_n M_n\left(\hat{c}^\dagger_{n\uparrow}\hat{c}_{n\uparrow} - \hat{c}^\dagger_{n\downarrow}\hat{c}_{n\downarrow}\right) \quad (2)$$

where $\hat{c}^\dagger_{n\sigma}$ creates an electron with spin σ at site n and μ is the chemical potential. The staggering is included in $M_n = (-1)^{\mathbf{n}} M$. The strength of the antiferromagnetic and superconducting coupling is given by M and Δ, respectively.
The Hamiltonian $\hat{H}^0 + \hat{H}^{int}$ is a simple mean-field lattice model to describe the phenomenology of the coexistence of d-wave superconducting and antiferromagnetic regions. This approach is similar to the starting point of many recent Bogoliubov-de Gennes calculations[12,13,21]. The Hamiltonian in Eqn. (1)-(2) can be viewed as the mean-field Hamiltonian of a $t-U-V$ Hubbard model, where the nearest neighbor attraction V gives rise to the d-wave superconductivity. In contrast the on-site Coulomb repulsion U only causes the antiferromagnetism. In this article we do not diagonalize $\hat{H}$ in the Bogoliubov-de Gennes scheme since such lattice calculations require unrealistically large gap Δ and magnetic field values. Instead we solve the Dyson equation exactly by inverting a large matrix. This approach has previously been utilized extensively to study various short-ranged impurity effects in superconductors[33], but can also be used for extended perturbations embedded in a $\hat{G}_0$ medium. Here $\hat{G}_0$ is the Green's function of the parent medium, in this case a d-wave BCS superconductor. This Green's function is given by

$$\hat{G}_0^{-1}(\mathbf{p},\omega) = (\omega + i\delta)\tau_0 - \xi_{\mathbf{p}}\tau_3 - \Delta_{\mathbf{p}}\tau_1 \quad (3)$$

where τ_ν denote the Pauli matrices in Nambu space and the gap function $\Delta_{\mathbf{p}} = \frac{\Delta_0}{2}(\cos(p_x) - \cos(p_y))$. The lattice constant a_0 is set to unity and $\xi_{\mathbf{p}} = \epsilon_{\mathbf{p}} - \mu$ with

$$\epsilon_{\mathbf{p}} = -2t(\cos(p_x) + \cos(p_y)) - 4t'(\cos(p_x)\cos(p_y)). \quad (4)$$

Here $t(t')$ refers to the nearest (next-nearest) neighbor hopping integral and μ is the chemical potential. We perform the 2D Fourier transform of $G_0(\mathbf{p},\omega)$ numerically by utilizing a real space lattice of 1000×1000 sites and a quasiparticle energy broadning of $\delta = 1.0$meV.
To simulate the situation around optimal doping of the hole doped cuprates the following parameters are chosen: $t = 300$meV, $t' = -120$meV, $\Delta_0 = 25$meV, $\mu = -354$meV. When the real space domain affected

by H^{int} involves a finite number of lattice sites $N \times N$ we can solve the Dyson equation exactly to find the full Greens function. Writing the Dyson equation in terms of real-space (and Nambu) matrices it becomes

$$\underline{\underline{G}}(\omega) = \underline{\underline{G}}^0(\omega)\left(\underline{\underline{1}} - \underline{\underline{H}}^{int}\underline{\underline{G}}^0(\omega)\right)^{-1}. \quad (5)$$

The size of the matrix $\left(\underline{\underline{1}} - \underline{\underline{H}}^{int}\underline{\underline{G}}^0(\omega)\right)$ is given by $(d \times N^2) \times (d \times N^2)$ where d is an integer equal to the number of components in the Nambu particle-hole spinor and N denotes the total number of lattice sites affected by the magnetic perturbation. Therefore a real-space lattice with 25×25 sites affected by perturbations results in a (1250×1250) matrix to be inverted.

Knowing the full Greens function we obtain the LDOS $\rho(\mathbf{r},\omega) = -\frac{1}{\pi}\mathrm{Im}\left[G_{11}(\mathbf{r},\omega) + G_{22}(\mathbf{r},-\omega)\right]$, which is proportional to the differential conductance measured in the STM experiments.

We have checked that the above approach reproduces the expected LDOS for unitary non-magnetic impurities in d-wave superconductors[30]. Also in this one-impurity case we reproduce the constant-energy LDOS maps recently calculated by Wang *et al.*[31,32]

Motivated by the qualitative agreement of the spin structure in figure 2a with the neutron data, we assume that this represents the induced magnetism around the vortices and calculate the LDOS in this striped environment. To this end we simply restrict the sum in Eqn. (2) to include the sites within these magnetic regions. The system is depicted in figure 2a where the grey background reveals the underlying superconducting state. Again the black (white) squares correspond to the sites affected by the staggered magnetic perturbation.

Figures 3 and 4 show real-space maps of the LDOS summed over a small energy window from -12 meV to +12 meV in intervals of 1meV for different strengths of the antiferromagnetic perturbation M. The vortex center is located in the center of the images. Figure 3 (4) is calculated with (without) the antiphase modulation of the adjacent stripes. Thus the spin configuration of figure 2a corresponds to the images in figure 3. The clear difference between the LDOS images of figures 3 and 4 reveals that the STM technique can be used to determine this phase relation. It is clearly seen from both figures 3 and 4 that the low energy LDOS structure eventually becomes ringshaped as the magnitude of M increases. In this limit the pinned stripes operate as steep potential walls. Figures 3a and 3b seem to display the closest resemblence to the experimental data[15] which indicates that the induced magnetism is very weak. In figure 5 we show the Fourier transform of several constant energy LDOS images for $M = 100$ meV with the antiphase spin modulation included. In these figures the Fourier component $\mathbf{q} = \mathbf{0}$ is located at the center. The detailed energy dependence of these images is caused by quasiparticle interference effects as pointed out by Wang *et al.*[31] in the case of a single impurity.

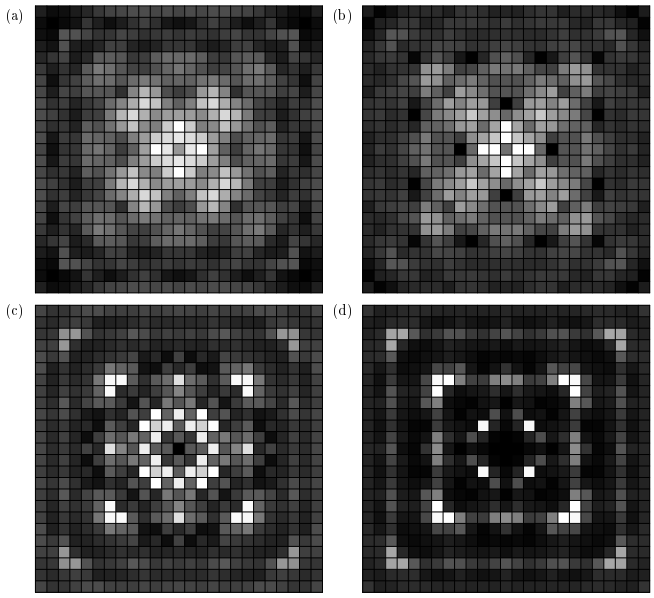


FIG. 3. Real-space LDOS summed from -12 meV to +12 meV for: a) M = 35 meV, b) M = 100 meV, c) M = 200 meV, d) M = 300 meV.

The dispersive features of the images presented in figure 5 are dependent on the microscopic parameters and the associated Fermi surface. However, it is also evident that the ringshaped stripes surrounding the vortex cores give rise to non-dispersive intensity around $\mathbf{q} = \frac{2\pi}{a_0}(\pm 1/4, 0)$ and $\mathbf{q} = \frac{2\pi}{a_0}(0, \pm 1/4)$. This in turn leads to the checkerboard pattern in the low energy sums of the LDOS displayed in figures 3 and 4 whereas the dispersive features fade away in these summed LDOS images[27].

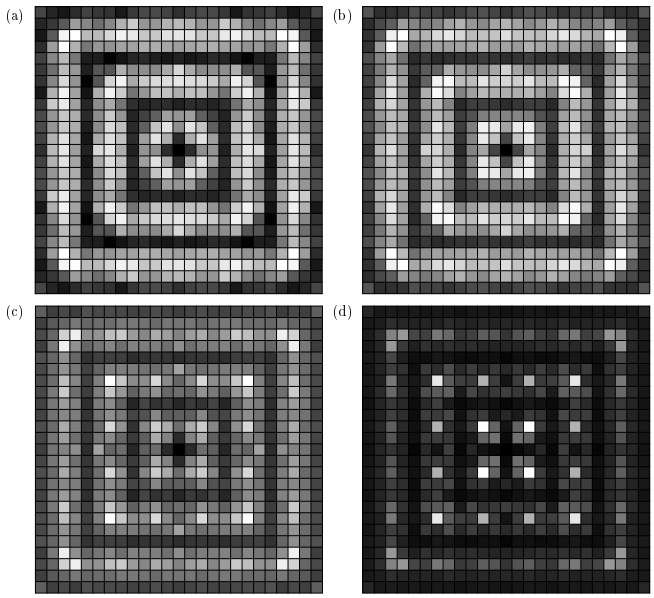


FIG. 4. Real-space LDOS summed from -12 meV to +12 meV for: a) M = 35 meV, b) M = 100 meV, c) M = 200 meV, d) M = 300 meV.

We have confirmed this fact by identifying similar non-dispersive features in the LDOS around configurations with different periodicities. For instance a structure with $2a_0$ charge periodicity leads to non-dispersive intensity around $\mathbf{q} = \frac{2\pi}{a_0}(\pm 1/2, 0)$ and $\mathbf{q} = \frac{2\pi}{a_0}(0, \pm 1/2)$.

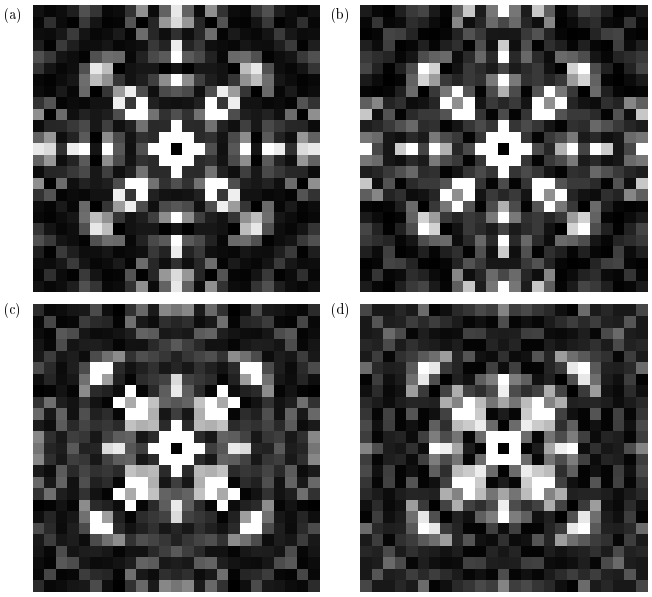


FIG. 5. Fourier images of the constant energy LDOS maps for M = 100 meV and a) ω = 3 meV, b) ω = 6 meV, c) ω = 9 meV, d) ω = 12 meV.

In the above calculation we have not yet included the Doppler shift from the circulating supercurrents or the gap suppression close to the vortex core. As pointed out by Polkovnikov *et al.*[18] the former effect is not expected to produce significant changes of the four-period modulations. As for the latter we have checked that a gap suppression only leads to minor quantitative changes in the dispersive part of the LDOS. Finally, Podolsky *et al.*[34] discussed scenarios of weak translational symmetry breaking and found that in order to explain quantitatively the *zero-field* STM results by Howald *et al.*[27] one needs to include dimerization, the modulation of the electron hopping. This dimerization will also produce quantitative changes, but not alter the qualitative conclusion that pinned stripes produce checkerboard LDOS.

In summary we have discussed the phenomenology of a simple physical picture of pinned stripes around vortex cores which are forced to be antiferromagnetic by an applied magnetic field. The induction of magnetic striped race-tracks around the core is consistent with the neutron diffraction spectra observed on LSCO with a doping level near x=0.10. As expected this is only true if the stripes are out of phase with their neighbors in the usual sense. In materials where a checkerboard spin pattern is relevant (possibly Bi2212 or overdoped LSCO), we show that a 45 degree rotation of the main incommensurable peaks is to be expected. Finally we studied the electronic structure around the vortices and identified a non-dispersive feature in the LDOS arising from the induced static antiferromagnetism. This feature gives rise to the checkerboard LDOS observed experimentally by Hoffman *et al.*[15] Thus both the STM measurements and the enhanced intensity of the incommensurable peaks observed by neutron diffraction can be ascribed to the phenomena of a single CuO_2 plane.

Acknowledgement: Support by the Danish Natural Science Research Council, Ole Rømer Grant No. 9600548.

[1] J. Zaanan, O. Gunnarson, Phys. Rev. B **40**, 7391 (1989).
[2] V.J. Emery and S.A. Kivelson, Physica C, **209**,597 (1993).
[3] S.A. Kivelson, E. Fradkin, V.J. Emery, Nature **393**, 550 (1998); V.J. Emery, S.A. Kivelson, J.M. Tranquada, Proc. Natl. Acad. Sci. U.S.A. **96**, 8814 (1999).
[4] S.R. White and D.J. Scalapino, Phys. Rev. Lett. **81**, 3227 (1998).
[5] M. Vojta, S. Sachdev, Phys. Rev. Lett. **83**, 3916 (1999).
[6] B.Lake *et al.*, Nature **415**, 299 (2002).
[7] B. Khaykovich *et al.*, Phys. Rev. B **66**, 014528 (2002).
[8] K. Kakuyanagi *et al.* cond-mat/0206362.
[9] R.I. Miller *et al.*, Phys. Rev. Lett. **88**, 137002 (2002).
[10] I. Maggio-Aprile *et al.*, Phys. Rev. Lett **75**, 2754 (1995); C. Renner *et al.*, Phys. Rev. Lett **80**, 3606 (1998).
[11] S.H. Pan *et al.* Phys. Rev. Lett. **85**, 1536 (2000).
[12] B.M. Andersen, H. Bruus, P. Hedegård, Phys. Rev. B **61**, 6298 (2000).
[13] J-X. Zhu, C.S. Ting, Phys. Rev. Lett **87**, 147002 (2001).
[14] A. Ghosal, C. Kallin, A.J. Berlinsky, cond-mat/0206414.
[15] J.E. Hoffman *et al.*, Science **295**, 466 (2002).
[16] D.P. Arovas *et al.*, Phys. Rev. Lett. **79**, 2871 (1997).
[17] E. Demler, S. Sachdev, Y. Zhang, Phys. Rev. Lett. **87**, 067202 (2001).
[18] A. Polkovnikov, M. Vojta, S. Sachdev, Phys. Rev. B **65**, 220509 (2002).
[19] H.D. Chen *et al.*, Phys. Rev. Lett **89**, 137004 (2002).
[20] A. Polkovnikov, S. Sachdev, M. Vojta, cond-mat/0208334.
[21] Y. Chen and C.S. Ting, Phys. Rev. B **65** 180513 (2002), Y. Chen, H.Y. Chen and C.S. Ting, cond-mat/0203283.
[22] M. Franz, D.E. Sheeny and Z. Tesanovic, Phys. Rev. Lett. **88**, 257005 (2002).
[23] J-X. Zhu, I. Martin and A.R. Bishop, Phys. Rev. Lett. **89** 067003 (2002).
[24] B.M. Andersen and P. Hedegård, cond-mat/0206502.
[25] S. Wakimoto *et al.*, Phys. Rev. B **60**, R769 (1999).
[26] M. Veilette *et al.*, Phys. Rev. Lett. **83**, 2413 (1999).
[27] C. Howald *et al.*, cond-mat/0201546; cond-mat/0208442.
[28] J.M. Tranquada *et al.*, Nature **375**, 561 (2002).
[29] O. Zachar, S.A. Kivelson, V.J.Emery, Phys. Rev. B **57**, 1422 (1998).
[30] A.V. Balatsky, M.I. Salkola and A. Rosengren, Phys. Rev. B **51**, 15547 (1995).
[31] Q.-H. Wang and D.-H. Lee, cond-mat/0205118.
[32] Naturally the full agreement is only obtained when using the same quasiparticle energy $\xi_{\mathbf{p}}$ as Wang *et al.*[31]
[33] M.E. Flatte and J.M. Byers, Phys. Rev. Lett. **80**, 4546 (1998); Phys. Rev. B **56**, 11213 (1997).
[34] D. Podolsky *et al.*, cond-mat/0204011.